Biol Blood Marrow Transplant 20 (2014) 1121–1128

Clinical Research

Pharmacokinetic and Pharmacodynamic Analysis of Inosine Monophosphate Dehydrogenase Activity in Hematopoietic Cell Transplantation Recipients Treated with Mycophenolate Mofetil

Hong Li [1], Donald E. Mager [1], Brenda M. Sandmaier [2,3], Barry E. Storer [2], Michael J. Boeckh [2,3], Meagan J. Bemer [4], Brian R. Phillips [4], Linda J. Risler [4], Jeannine S. McCune [2,4,*]

[1] *Department of Pharmaceutical Sciences, University at Buffalo, SUNY, Buffalo, New York*
[2] *Clinical Research Division, Fred Hutchinson Cancer Research Center, Seattle, Washington*
[3] *Schools of Medicine, University of Washington, Seattle, Washington*
[4] *School of Pharmacy, University of Washington, Seattle, Washington*

Article history:
Received 12 February 2014
Accepted 31 March 2014

Key Words:
Mycophenolic acid
Therapeutic drug monitoring
Population pharmacokinetics
Limited sampling schedule
Hematopoietic cell transplantation
Covariates
Albumin
Cyclosporine

A B S T R A C T

A novel approach to personalizing postgrafting immunosuppression in hematopoietic cell transplantation (HCT) recipients is evaluating inosine monophosphate dehydrogenase (IMPDH) activity as a drug-specific biomarker of mycophenolic acid (MPA)-induced immunosuppression. This prospective study evaluated total MPA, unbound MPA, and total MPA glucuronide plasma concentrations and IMPDH activity in peripheral blood mononuclear cells (PMNCs) at 5 time points after the morning dose of oral mycophenolate mofetil (MMF) on day +21 in 56 nonmyeloablative HCT recipients. Substantial interpatient variability in pharmacokinetics and pharmacodynamics was observed and accurately characterized by the population pharmacokinetic-dynamic model. IMPDH activity decreased with increasing MPA plasma concentration, with maximum inhibition coinciding with maximum MPA concentration in most patients. The overall relationship between MPA concentration and IMPDH activity was described by a direct inhibitory maximum effect model with an IC_{50} of 3.23 mg/L total MPA and 57.3 ng/mL unbound MPA. The day +21 IMPDH area under the effect curve (AUEC) was associated with cytomegalovirus reactivation, nonrelapse mortality, and overall mortality. In conclusion, a pharmacokinetic-dynamic model was developed that relates plasma MPA concentrations with PMNC IMPDH activity after an MMF dose in HCT recipients. Future studies should validate this model and confirm that day +21 IMPDH AUEC is a predictive biomarker.

INTRODUCTION

The availability of allogeneic hematopoietic cell transplantation (HCT) has expanded with the development of lower dose nonmyeloablative conditioning regimens, which depend on achieving a delicate balance between recipient and donor cells to obtain immunosuppression of the recipient, optimal antitumor effect, and minimal toxicity [1]. Nonmyeloablative HCT recipients often receive mycophenolate mofetil (MMF) and a calcineurin inhibitor (cyclosporine or tacrolimus) as postgrafting immunosuppression, which aims to facilitate allogeneic engraftment and control graft-versus-host disease (GVHD) [2,3].

There is considerable variability in the clinical outcomes of these patients. Some interpatient variability in clinical outcomes could, in part, reflect differences in each recipient's sensitivity to MMF. The pharmacokinetics and drug-specific pharmacodynamics of mycophenolic acid (MPA), the therapeutically active metabolite of MMF, are potential sources of this interindividual variability (IIV). MMF is rapidly hydrolyzed to MPA in the gastrointestinal tract. After rapid absorption, MPA undergoes hepatic metabolism by various UDP-glucuronosyltransferase isoenzymes to form MPA glucuronide (total MPAG) [4]. After oral MMF administration, there is considerable between-patient variability in total and unbound MPA area under the concentration-time curves (AUCs) [5,6]. The available pharmacodynamic data in allogeneic HCT recipients suggest a relationship between MPA AUC and clinical outcomes [7]. Although some HCT centers have proposed personalizing MMF doses based on MPA AUC [8], there is an ongoing debate regarding the benefits of such therapeutic drug monitoring in solid organ transplantation [9].

MPA is a selective, reversible, and noncompetitive inhibitor of inosine monophosphate dehydrogenase (IMPDH) [10]. IMPDH is the rate-limiting enzyme involved in the de novo synthesis of guanosine nucleotides; IMPDH catalyzes the oxidation of inosine 5′-monophosphate to xanthosine 5′-monophosphate (XMP) by a nicotinamide adenine dinucleotide positive–dependent reaction [11]. Characterizing the pharmacodynamic relationship between MPA and IMPDH activity is critical to understanding the potential benefit of alternative MMF dosing strategies in nonmyeloablative HCT recipients. Thus, we sought to characterize the pharmacokinetic-dynamic relationship between

Financial disclosure: See Acknowledgments on page 1128.

* Correspondence and reprint requests: Jeannine S. McCune, PharmD, Department of Pharmacy, Box 357630, University of Washington, Seattle, WA 98195.
E-mail address: jmccune@fhcrc.org (J.S. McCune).

1083-8791/$ – see front matter © 2014 American Society for Blood and Marrow Transplantation.
http://dx.doi.org/10.1016/j.bbmt.2014.03.032

total and unbound MPA plasma concentrations and ex vivo IMPDH activity in peripheral blood mononuclear cells (PMNCs) in nonmyeloblative HCT recipients receiving MMF as postgrafting immunosuppression.

METHODS

Patient Characteristics

Between November 2008 and February 2012, 105 patients participated in a prospective ancillary biomarker study in nonmyeloablative allogeneic HCT recipients. Study participation influenced neither the conditioning regimen nor postgrafting immunosuppression. Patients (age > 18 years) receiving fludarabine monophosphate (Fludara; Berlex, Montville, NJ) and total body irradiation conditioning, a related or unrelated donor granulocyte colony-stimulating factor–mobilized peripheral blood mononuclear cell (G-PBMC) graft, and postgrafting immuosuppression with a calcineurin inhibitor (cyclosporine or tacrolimus) and MMF were eligible for recruitment in this study. One participant received both G-PBMCs and bone marrow because of inadequate G-PBMC yield from the donor's apheresis. The choice and kinetics-based dose targeting of the calcineurin inhibitor were determined by the HCT protocol. In addition to cyclosporine or tacrolimus, some participants also received sirolimus as part of their postgrafting immunosuppression.

Exclusion criteria included diagnosis of an immunodeficiency disorder or scheduled to receive immunosuppression in addition to fludarabine/total body irradiation (eg, alemtuzumab, thymoglobulin) during HCT conditioning to day +28 after graft infusion. This protocol was approved by the Institutional Review Board at the Fred Hutchinson Cancer Research Center (FHCRC Protocol 1980, Clinicaltrials.gov NCT00764829). Written informed consent was obtained from all patients before study participation.

The MMF dose and administration frequency were specified by the HCT protocol. MMF doses were based on body weight and rounded to the nearest 250-mg dose, as previously described [6]. MMF doses were not adjusted based on MPA plasma concentrations or IMPDH determinations.

This cohort was divided into 2 separate datasets, the development dataset and the validation dataset. The development dataset was used to develop the pharmacokinetic/dynamic model relating plasma MPA concentrations with PMNC IMPDH activity and to validate our previous population pharmacokinetic model [5,6]. The validation dataset was used to validate the pharmacokinetic/dynamic model relating plasma MPA concentrations and PMNC IMPDH. The patient characteristics of the development and validation datasets are shown in Table 1.

Sample Collection

Peripheral blood samples (8 mL drawn into EDTA vacutainers, Supplemental Figure 1) were obtained on day +21. The total MPA, unbound MPA, and total MPAG plasma concentrations and IMPDH activity in PMNCs were quantitated in each sample. All assays were performed on each of the samples. Of the 56 AUCs, 2 were collected on day +19, 17 on day +20, 32 on day +21, 3 on day +22, 1 on day +23, and 1 on day +25. Samples were drawn before and 1, 2, 2.5, and 6 hours after oral MMF for 29 patients (November 2008 to March 2011; development and validation cohorts) and before and 1.25, 2, 3, and 4 hours after oral MMF for 27 patients (April 2011 to February 2012, validation cohort). These patients were primarily treated in the ambulatory clinic, and therefore limited sampling schedules were used to maximize compliance. From November 2008 to March 2011, compliance for pharmacokinetic samples was 63% (41 of 65 participants); this decreased to 50% (6 of 12 participants) when participants were paid per AUC obtained. In April 2011, the sampling schedule was shortened to 4 hours after the oral MMF dose based on a prior analysis [6]. With this change, complaince improved to 76% (26 of 34 participants). In 50 of 56 participants, all 5 samples were collected. Among the remaining participants, 2 had 1 sample collected, 1 had 3 samples collected, 2 had 4 samples collected, and 1 had 6 samples collected. IMPDH activity on day +2 after HCT was planned; this could not be conducted, however, due to myelosuppression resulting from the conditioning regimen.

Table 1 lists the participant characteristics, including biochemistry values and concomitant medications associated with MPA pharmacokinetic parameters. Our previous population pharmacokinetic model after intravenous or oral MMF administration indicated that MPA clearance was significantly increased (by 33.8%) with concomitant cyclosporine and negatively correlated with albumin concentration [6].

Reagents and Chemicals

All nucleotides used as substrates for the enzymatic assay or as chromatographic standards were obtained from Sigma (St. Louis, MO). Nicotinamide adenine dinucleotide was also purchased from Sigma. Acetonitrile, ammonium acetate, methanol, sodium hydroxide, sodium phosphate monobasic, ammonium acetate, ammonium hydroxide, and potassium chloride were all purchased from Thermo Fisher (Waltham, MA). Dulbecco's PBS was purchased from Invitrogen (Grand Island, NY). Ficoll Hypaque solution (density 1.077 g/mL) was obtained from GE Healthcare (Uppsala, Sweden).

Quantitation of MPA and Total MPAG

Each plasma sample was analyzed for total MPA, unbound MPA, and total MPAG plasma concentrations using reverse phase HPLC with mass

Table 1
Participant Characteristics

	Development Dataset	Validation Dataset	Overall
Number of participants	34	22	56
Female/male gender (% male)	14/20 (59%)	7/15 (68%)	21/35 (63%)
Recipients' ages, yr	63 (28-72)	58 (26-73)	62 (26-73)
Adjusted ideal body weight, kg	70.6 (44.3-88.8)	71.2 (44.4-93.4)	70.7 (44.3-93.4)
Height, cm	172 (149-184)	173 (147-194)	172 (147-194)
Body surface area, m^2	1.96 (1.40-2.60)	1.95 (1.50-2.47)	1.95 (1.40-2.60)
Donor type, related/unrelated (% related)	6/28 (18%)	5/17 (23%)*	11/45 (20%)
Female donor to male recipient	7 (21%)	8 (36%)	15 (27%)
Kahl relapse risk			
Low	13 (38%)	6 (27%)	19 (34%)
Standard	13 (38%)	13 (59%)	26 (46%)
High	8 (24%)	3 (14%)	11 (20%)
Covariates associated with MPA clearance			
Concomitant calcineurin inhibitor†			
Cyclosporine	25 (74%)	18 (82%)	43 (77%)
Tacrolimus	9 (26%)	4 (18%)	13 (23%)
Serum creatinine (mg/dL)	1.1 (.6-2.0)	1.2 (.7-2.2)	1.1 (.6-2.2)
Serum albumin (g/dL)	3.4 (2.1-4.2)	3.5 (2.4-4.1)	3.4 (2.1-4.2)
Pharmacokinetic sampling around morning MMF dose on day +21‡			
Before and 1, 2, 2.5, 6 h§	29 (85%)	0	29 (52%)
Before and 1.25, 2, 3, 4 h‖	5 (15%)	22 (100%)	27 (48%)
Day +28 donor T cell chimerism	85% (35-100)	95% (61-100)	89% (35-100)

Categorical data presented as number (percentage) of participants meeting stated criteria; continuous data presented as median (min-max).

* Three patients (1 related, 2 unrelated donor) had antigen-level mismatch.

† Concomitant sirolimus in 8 cyclosporine and 3 tacrolimus patients (see Patient Characteristics in Methods).

‡ Modified to improve patient adherence (see Sample Collection in Methods).

§ November 2008 to March 2011.

‖ April 2011 to February 2012.

spectrometry (MS) detection. For total MPA and total MPAG quantitation, plasma samples (100 μL) with the internal standard (20 μL MPA-d3 and MPA β-D-glucuronide-d3) were combined with 50 μL methanol and 1000 μL acetonitrile, vortexed, and subsequently centrifuged. The supernatant (1 μL) was injected onto a light chromatography (LC)/MS running a gradient of 2.0 mM ammonium formate (pH 3.3) and acetonitrile through an Agilent C18 column (2.1 mm × 150 mm × 5 μm; Agilent Technologies, Palo Alto, CA). Monitored ions included *m/z* 321 for the $(M+H^+)$ ion of MPA, *m/z* 324 for the $(M+H^+)$ ion of MPA-d3 (internal standard), *m/z* 495.2 for the $(M+H^+)$ ion of total MPAG, and *m/z* 498.1 for the $(M+H^+)$ ion of total MPAG-d3 (internal standard). The dynamic range was .3 to 15.5 mg/L for MPA and .21.5 to 215 mg/L for total MPAG. The interday coefficient of variation was less than 10.7%.

Unbound MPA plasma concentrations were determined by equilibrium dialysis using Pierce rapid equilibrium dialysis devices (Thermo Fisher). After incubation and processing of plasma samples according to Pierce rapid equilibrium dialysis manufacturer instructions, samples were analyzed using LC/MS as above with slight modifications (ie, mobile phase was an isocratic mixture of 55% 2.0 mM ammonium formate [pH 3.3] and 45% acetonitrile, with a total run time was 5 minutes). The percentage of unbound (free) MPA was calculated as follows: unbound MPA = 100 × (1-bound MPA).

Isolation of Human PMNCs and IMPDH Activity Assay

PMNCs were isolated within 6 hours of collection by diluting blood in PBS at a 1:1 v:v ratio and subsequently layering on top of Ficoll as previously described [12]. In brief, PMNCs were collected, diluted to 10 mL with PBS to wash, and centrifuged. The cell counts were quantitated using a Horiba Diagnostics ABX Micro 60 (Irving, CA), and distilled water was added to the supernatant to adjust the cell concentration to $.5 \times 10^6$ cells/mL lysate. This PMNC count was used to standardize the IMPDH activity measurement. After storage at −80°C, the IMPDH activity was determined from the conversion of inosine monophosphate to XMP according to procedures adapted from Glander et al. [13] and Daxecker et al. [14]. The incubation reaction mixture included NaH_2PO_4, KCl, inosine monophosphate (.8 mL of 6.0 mmol/L) and nicotinamide adenine dinucleotide (.8 mL of 4.5 mmol/L, made fresh each day). The incubation reaction was started via the addition of the reaction mixture to 50 μL prewarmed cell lysate (standard concentration of $.5 \times 10^6$ cells/mL).

For each incubation, the enzymatic reaction was terminated after 2.5 hours of incubation by the addition of methanol followed by internal standard (8-bromo adenosine 5′-monophosphate), processed, and injected on the LC/MS running a gradient of .1 M ammonium acetate (pH 8.5) and acetonitrile through a Thermo Scientific Hypercarb column (2.0 mm × 100 mm × 5 μm, part no. 35005-102130; Thermo Scientific, Bellefonte, PA). An Agilent G1946D mass selective detection (Agilent Technologies) atmospheric pressure ionization-electrospray in positive ion mode was used. The mass selective detection was run in the selected ion monitoring mode. Monitored ions included *m/z* 365 for the $(M+H^+)$ ion of XMP, *m/z* 348 for the $(M+H^+)$ ion of adenosine monophosphate, and *m/z* 426 for the $(M+H^+)$ ion of 8-bromo adenosine 5′-monophosphate, the internal standard. Typical retention times were 4.3 minutes for XMP, 5.1 minutes for inosine monophosphate, and 7.0 minutes for 8-bromo adenosine 5′-monophosphate. The limit of quantification (signal-to-noise ratio > 60 and coefficient of variation < 2%) was 58 pmol.

A quality control pooled lysate obtained from the PMNCs of healthy subjects was run in triplicate with every incubation. The coefficient of variation for the control lysate was 6.2% over 39 incubations. Each PMNC sample was run in triplicate; the average of the triplicates is reported as the IMPDH activity. IMPDH activity is standardized to the ex vivo PMNC count determined after Ficoll isolation and expressed as pmol XMP/10^6 cells/h.

MPA Population Pharmacokinetic-Dynamic Analysis

Pharmacokinetic (total MPA, unbound MPA, and total MPAG plasma concentrations) and pharmacodynamic (XMP formation in PMNCs to provide IMPDH activity) data were available at each concentration time point. The pharmacokinetic-dynamic models were developed in a sequential manner: the pharmacokinetic model was developed first, then each participant's pharmacokinetic parameters were fixed for the creation of the pharmacodynamic model.

The initial pharmacokinetic model of Li et al. [6], which was developed in 402 HCT recipients, was modified to include total MPAG (as described by Musuamba et al. [15]) and unbound MPA concentrations. Briefly, total MPA pharmacokinetics was described using a 2-compartmental model with first-order elimination and first-order absorption with a lag time (Figure 1). The model was parameterized as clearance (CL), volume of the central compartment (V_c), volume of the peripheral compartment (V_p), and intercompartment clearance (Q). Total MPAG pharmacokinetics was described

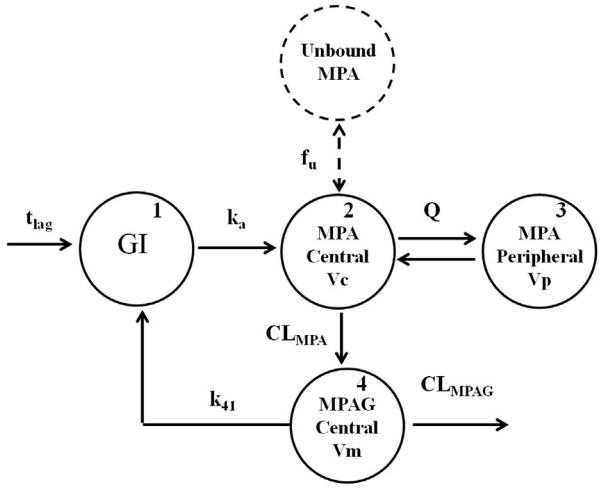

Figure 1. Final pharmacokinetic model characterizing total MPA, unbound MPA, and total MPAG concentrations following oral MMF administration. t_{lag}, lag time; GI, gastrointestinal tract; k_a, first-order absorption rate constant; f_u, fraction unbound of MPA; V_c, volume of central compartment of total MPA; Q, intercompartment clearance of total MPA; V_p, volume of peripheral compartment of total MPA; CL_{MPA}, clearance of total MPA; CL_{MPAG}, clearance of total MPAG; V_m, volume of central compartment of total MPAG; k_{41}, first-order rate constant of EHC.

using a 1-compartmental model with first-order elimination. It was assumed that MPA is metabolized to total MPAG by a first-order process and that 100% of MPA is converted to total MPAG because urinary MPA data were not available. Collection of urinary excretion data was not possible because participants were treated in the ambulatory clinic. Therefore, total MPAG CL and V_d are apparent clearance and volume of distribution (ie, CL/f_m and V/f_m). Enterohepatic recirculation (EHC) of total MPAG was represented as a first-order process between the total MPAG central compartment and the gastrointestinal tract. Unbound MPA concentrations were modeled as $[MPA_{unbound}] = [MPA_{total}] \times f_u$, with $[MPA_{unbound}]$, $[MPA_{total}]$, and f_u representing unbound MPA concentration, total MPA concentration, and the unbound fraction, respectively.

We also sought to validate the covariate effect of the calcineurin inhibitor (cyclosporine or tacrolimus) on MPA clearance [5,6]. MPA clearance was eventually defined by the following equation:

$$\text{MPA CL} = 24.2 \times \left(\frac{\text{body weight}}{70}\right)^{.75} \times \left(\frac{\text{albumin}}{3.4}\right)^{-.686} \times (1 + .338 \times \text{CSP}) \quad \text{(Eq. 1)}$$

with body weight in kg, albumin in g/dL, and CSP = 1 for cyclosporine and 0 for tacrolimus.

The Bayesian total MPA $AUC_{0\text{-}8h}$ of 27 participants who received MMF every 8 hours was calculated. The AUCs of patients receiving concomitant tacrolimus were compared with those of patients taking cyclosporine. In addition, this simulation was executed using population mean parameter estimates to compare total MPA $AUC_{0\text{-}12h}$ in patients receiving either concomitant cyclosporine or tacrolimus. Both Bayesian estimations and simulations were performed using NONMEM VII (Icon Development Solutions, LLC, Ellicott City, MD).

Subsequent to finalization of the population pharmacokinetic model, the relationship between MPA concentrations and IMPDH activity was explored graphically and modeled using an inhibitory maximum effect model:

$$E = E_0 \times \left(1 - \frac{I_{max} \bullet C_p^{\gamma}}{IC_{50}^{\gamma} + C_p^{\gamma}}\right) \quad \text{(Eq. 2)}$$

with E_0 as baseline IMPDH activity (minimal inhibition), I_{max} as maximal IMPDH inhibition, C_p as the MPA plasma concentration, IC_{50} as the MPA concentration that causes 50% of maximal IMPDH inhibition, and γ as the Hill coefficient that governs the slope of MPA concentration versus IMPDH activity.

Population pharmacokinetic-dynamic analysis was performed using nonlinear mixed effects modeling (NONMEM® VII .1.0). The Monte Carlo Important Sampling expectation maximization method was used throughout the modeling process. Pharmacokinetic models were simultaneously fitted to total MPA, unbound MPA, and total MPAG plasma concentrations. MMF dose and total MPAG concentration were multiplied by

.739 and .594, respectively, to convert these values to their equivalent MPA values [16]. Clearance and volume of distribution were allometrically scaled to body weight with exponents fixed to .75 and 1, respectively. Between-subject variability was modeled using an exponential error model. Pharmacokinetic data were log-transformed, and an additive error model was applied to describe residual error. A proportional error model was used for pharmacodynamic residual error.

Stepwise forward selection and backward elimination, based on the likelihood ratio test and a prespecified alpha level, were applied across the base, intermediate, and final models [5]. A covariate was included in the intermediate model when a decrease of at least 6.6 in the objective function value ($P < .01$) occurred. A covariate was retained in the final model when an increase of at least 10.8 in objective function value ($P < .001$) occurred when this covariate was removed. The tested covariates included age, body surface area, serum albumin, blood urea nitrogen, serum creatinine, creatinine clearance, alkaline phosphatase, alanine aminotransferase, aspartate aminotransferase, lactate dehydrogenase, total bilirubin, and direct bilirubin. All biochemistry values were obtained within 7 days before the pharmacokinetic-dynamic sampling.

Model Validation

The pharmacokinetic-dynamic model was validated internally and externally. Goodness-of-fit and visual predictive check plots were used for internal validation. Goodness-of-fit plots included observed versus predicted concentrations as well as conditional weighted residuals versus model predictions and time after dose. For visual predictive check plots, 500 datasets were simulated from parameter estimates of the final model, and the 5th, 50th, and 95th percentiles of simulated data were compared with observed data.

External validation was carried out using 2 methods: predicting observed pharmacokinetic-dynamic data in the validation dataset (n = 22 participants) and comparing results of Monte Carlo simulations to the observed data. Using the population model developed from the development dataset, predicted concentrations (both population and Bayesian predictions) were calculated for each participant in the validation dataset, using the known MMF dosing history and available pharmacokinetic sampling times. Predictions were obtained by setting POSTHOC and MAXEVAL = 0 options in the NONMEM $ESTIMATION command. Bias in model prediction was assessed by calculating the percent mean prediction error (MPE%) as follows:

$$\mathrm{MPE\%(PRED)} = \left(\frac{1}{N}\sum_{i=1}^{n}\frac{\mathrm{PRED-OBS}}{\mathrm{OBS}}\right)\times 100 \quad \text{(Eq. 3)}$$

$$\mathrm{MPE\%(IPRE)} = \left(\frac{1}{N}\sum_{i=1}^{n}\frac{\mathrm{IPRE-OBS}}{\mathrm{OBS}}\right)\times 100 \quad \text{(Eq. 4)}$$

where PRED and IPRE are population prediction and individual (Bayesian) predictions, respectively, and OBS represents the observed data of the participants in the validation dataset. The Monte Carlo simulation approach generated a total of 100 studies of 22 participants. Simulations combined estimated pharmacokinetic-dynamic parameters from the development dataset with participant characteristics, dosing, and sampling information from the validation dataset. The median, 5th, and 95th percentiles of simulated data were plotted alongside the corresponding median, 5th, and 95th percentiles of observed data. This simulation was performed in NONMEM VII. Plots and statistical analysis were performed in S-PLUS 8.0 (Insightful Corp, Seattle, WA) or the open-source statistical software R (version 2.10.0; R Foundation for Statistical Computing, Vienna, Austria; available at: http://www.R-project.org).

Clinical Outcomes

The area under the effect–time curve (AUEC, pmol × 10^6 cells) for IMPDH activity was calculated for the statistical analysis with clinical outcomes. Specifically, the participant's predose value for IMPDH activity was considered as baseline, and then the area below the baseline was calculated using noncompartmental analysis to provide the AUEC. Because the latest assessment of IMPDH AUEC occurred on day +25, analysis of clinical outcomes was restricted to events taking place on day +26 or later.

Clinical outcomes of interest were toxicity to MMF (ie, cytomegalovirus [CMV] reactivation), efficacy of MMF (ie, day +28 donor T cell chimerism, acute and chronic GVHD), and overall HCT outcomes (ie, relapse, nonrelapse mortality, and overall survival). For day +28 T cell chimerism: 9% had donor chimerism less than 50% and 32% had donor chimerism less than 75%. The median for day +28 donor T cell chimerism was 89% (range, 35% to 100%). Only 1 participant experienced graft rejection, so this was not evaluated.

Of the 56 participants, 12 (21%) were CMV positive with a CMV-positive donor, 21 (38%) were CMV positive with a CMV-negative donor, 8 (14%) were CMV negative with a CMV-positive donor, and 15 (27%) were CMV negative with a CMV-negative donor. When either the donor or recipient was CMV positive, the CMV antigenemia assay to detect CMV pp65 antigen was performed on a weekly basis for the first 3 months after HCT. Twenty-two participants experienced CMV reactivation post-transplant. Acute GVHD was graded as previously described [17]. Hematological diseases were classified as low, standard, or high risk of relapse per the Kahl criteria to evaluate relapse rate in a consistent manner [18]. We defined disease relapse or disease progression as disease recurrence after complete remission or progression of persistent disease. Clinical endpoints were measured to the time of last clinical follow-up. The median time to last clinical follow-up was 1.4 years (range, .3 to 3.3 years).

Statistical Analysis

IMPDH AUEC was treated as a fixed covariate. Cumulative incidence curves for acute GVHD were estimated using methods previously described [19]. Cox regression analysis was used to model the impact of IMPDH AUEC on time-to-event endpoints. Death and relapse were treated as competing risks for analysis of acute and chronic GVHD. Relapse was treated as a competing risk for the analysis of nonrelapse mortality. The effects of IMPDH AUEC on hazard ratios were expressed as the effect per doubling of IMPDH AUEC. All reported *P* values are 2-sided, and those estimated from regression models are derived from the Wald test. No adjustments were made for multiple comparisons.

RESULTS

Patient characteristics are summarized in Table 1. The dose, administration route, and administration frequency of MMF were determined by the participant's HCT transplant protocol.

Population Pharmacokinetic Model

A total of 167 pharmacokinetic samples (total MPA, unbound MPA, and total MPAG) was used for population pharmacokinetic model building. A previously developed MPA pharmacokinetic model was modified to include total MPAG EHC (Figure 1). Total MPAG was assumed to be excreted to the gastrointestinal tract by a continuous first-order process. It was estimated that 29.5% of MPA (ie, EHC % = $k_{41}/(k_{41} + CL_{TOTAL\ MPAG}/V_m)$) underwent EHC. Data fitting was significantly improved when EHC was only integrated with concomitant tacrolimus. The current dataset did not support a more physiologically based EHC model [20]. Of note, the lag time could not be estimated for each participant because his or her food intake was not available. The population mean of lag time was fixed to a previous estimate [5] because the sampling schedule was inadequate to estimate this parameter. Because of convolution of the absorption and distribution phases of MPA and the absence of intravenous data, V_p could not be identified and was fixed to a previously determined value [5]. Pharmacokinetic parameters were well estimated, as shown in Table 2. The visual predictive checks and the time courses of total MPA concentration, unbound MPA concentration, and total MPAG concentration are shown in Supplemental Figure 2.

Covariate analysis identified serum creatinine as a significant covariate of total MPAG CL. Inclusion of serum creatinine in the model resulted in a 24-unit decrease in objective function value and a 9.7% decrease in IIV of total MPAG CL. The final pharmacokinetic model included both cyclosporine and serum creatinine as model covariates. Goodness-of-fit plots are presented in Supplemental Figure 3.

Cyclosporine inhibits multidrug resistance-associated protein 2–mediated EHC of total MPAG and thus results in decreased MPA AUC and increased MPA clearance (Supplemental Figure 4). Median total MPA $AUC_{0\text{-}8h}$ was increased by 33% in participants receiving concomitant tacrolimus. In addition, simulations using population means demonstrated that the MPA $AUC_{0\text{-}12h}$ in participants taking

Table 2
Population Pharmacokinetic Analysis for Total MPA, Unbound MPA and Total MPAG Plasma Concentrations

Pharmacokinetic Model		Parameter Estimates (RSE%)	
Parameter	Explanation	Base Model	Final Model
k_a (h^{-1})	First-order rate constant representing both formation and absorption process	.913 (11.7)	.916 (12.4)
T_{lag} (h)	Lag time of oral absorption	.228 FIXED	.228 (21) FIXED
CL_{MPA} (L/h/70 kg)*	Clearance of total MPA	31.4 (5.6)	31.4 (5.7)
$CL_{TOTAL\ MPAG}$ (L/h/70 kg)†	Clearance of total MPAG	1.29 (7.2)	1.32 (5.9)
Q_{MPA} (L/h/70 kg)	Intercompartmental clearance of total MPA	11.6 (29.8)	11.5 (27.7)
k_{41} (L/h/70 kg)	First-order rate constant representing total MPAG EHC	.0503 (45.3)	.0558 (44.1)
V_c (L/70 kg)	Volume of central compartment of total MPA	25.3 (13.0)	26.5 (12.9)
V_p (L/70 kg)	Volume of peripheral compartment of total MPA	247 (21) FIXED	247 (21) FIXED
V_m/f_m (L/70 kg)	Volume of central compartment of total MPAG	9.91 (8.9)	9.91 (8.8)
f_u (%)	Fraction unbound of MPA	1.76 (2.6)	1.76 (2.7)
$\theta_{creatinine}$†	Power coefficient of creatinine covariate effect on total MPAG clearance	Not estimated (NE)	−.919 (19.5)
Interindividual variability‡			
k_a (CV%)		55.0 (35.1)	55.0 (42.2)
T_{lag} (CV%)		133.4 (24.7)	132.7 (25.9)
CL_{MPA} (CV%)		38.2 (21.2)	38.5 (21.4)
$CL_{TOTAL\ MPAG}$ (CV%)		53.7 (18.5)	44.0 (18.5)
Q (CV%)		162.8 (35.3)	161.2 (29.5)
k_{41} (CV%)		118.3 (70.7)	110.5 (65.7)
V_c (CV%)		47.1 (46.8)	47.0 (79.6)
V_p (CV%)		84.2 (49.5)	86.4 (109.2)
V_m/f_m (CV%)		44.4 (34.3)	45.1 (32.1)
f_u (CV%)		14.9 (31.8)	15.0 (33.0)
Residual variability§			
Total MPA		.20 (11.3)	.20 (11.8)
Unbound MPA		.20 (11.2)	.20 (11.8)
Total MPAG		.09 (11.9)	.09 (12.1)

CV indicates coefficient of variation; RSE, relative standard error; T_{lag}, lag time.
* Typical CL values were calculated as described in Eq. 1. Body weight calculations described in Patient Characteristics in Methods.
† $CL_{TOTAL\ MPAG}$, $CL_{pop} \times (\text{serum creatinine}/1.12)^{-.919}$.
‡ Bioavailability was fixed to 1.
§ Additive residual error was on a natural logarithmic-scale.

tacrolimus was, on average, 1.38-fold higher than in patients taking cyclosporine. Overall, these results confirmed our previous findings [6] and can be considered as an external validation for Eq. 1 where MPA CL is increased by 33.8% with concomitant cyclosporine.

Population Pharmacokinetic-Dynamic Model

For the pharmacodynamic analysis, 267 PMNC samples were available for ex vivo IMPDH activity quantitation. Of these, 263 samples had 3 replicates for IMPDH activity and 4 samples had 2 replicates. Within-sample variability was calculated by dividing the lowest XMP formation rate by the highest rate within each sample (ie, minimum/maximum). The within-sample variability ranged from 74% to 100%. Most replicates (257, 96%) had within-sample variability greater than 90%. For pharmacodynamic model building, there were 166 IMPDH activity measurements in the development dataset and 101 IMPDH activity measurements for the validation dataset.

The concentration-response relationships between MPA concentration (either total or unbound) and IMPDH activity are shown in Figure 2. IMPDH activity was inversely related to total MPA (Figure 2A) and unbound MPA (Figure 2B) concentrations. The greatest level of inhibition was associated with the greatest MPA concentration, after which IMPDH activity returned to near predose values. This association is shown for the entire population (Figure 2C) as mean plus standard deviation and also using each participant's predose MPA concentration and IMPDH activity as their own controls (Figure 2D). Maximum inhibition coincided with maximum MPA concentration, indicating a direct effect relationship. When analyzing all 267 pharmacokinetic-dynamic data points in the development dataset, the MPA concentration − IMPDH activity relationship could be well described by an inhibitory direct effect E_{max} model (Eq. 2). The final model-based IC_{50} estimate was 3.23 mg/L (relative standard error 10.7%; IIV 53.1%CV) for total MPA and 57.3 ng/mL (relative standard error 11.2%; IIV 56.3%CV) for unbound MPA. Maximum inhibition could not be estimated from the observed data and was therefore fixed to 1. The Hill coefficient was estimated to be close to 1 and was fixed to 1 in the final parameter estimation. Table 3 summarizes the estimated and fixed population pharmacodynamic parameters.

The final pharmacodynamic model did not include any of the available covariates. Age was negatively correlated with E_0, with a Pearson correlation of .25 ($P = .06$). Inclusion of age as a model covariate did not result in a significant improvement in model fitting, and age was thus not included in the final model. Notably, the calcineurin inhibitor and graft source (ie, related versus unrelated donor) did not affect the IC_{50} or E_0 (Supplemental Figure 5).

The final pharmacokinetic-dynamic parameter estimates were updated using a combination of both the model-building and validation datasets (Tables 2 and 3). Both visual predictive check and goodness-of-fit plots demonstrated that the final model precisely described the observed pharmacokinetic and pharmacodynamic data (Supplemental Figures 2 and 3).

Validation of the Population Pharmacokinetic-Dynamic Model

The participant characteristics were similar between the model-building and validation datasets (Table 1). Two methods were applied to the validation dataset to externally corroborate the developed population pharmacokinetic-dynamic model. The results from both methods

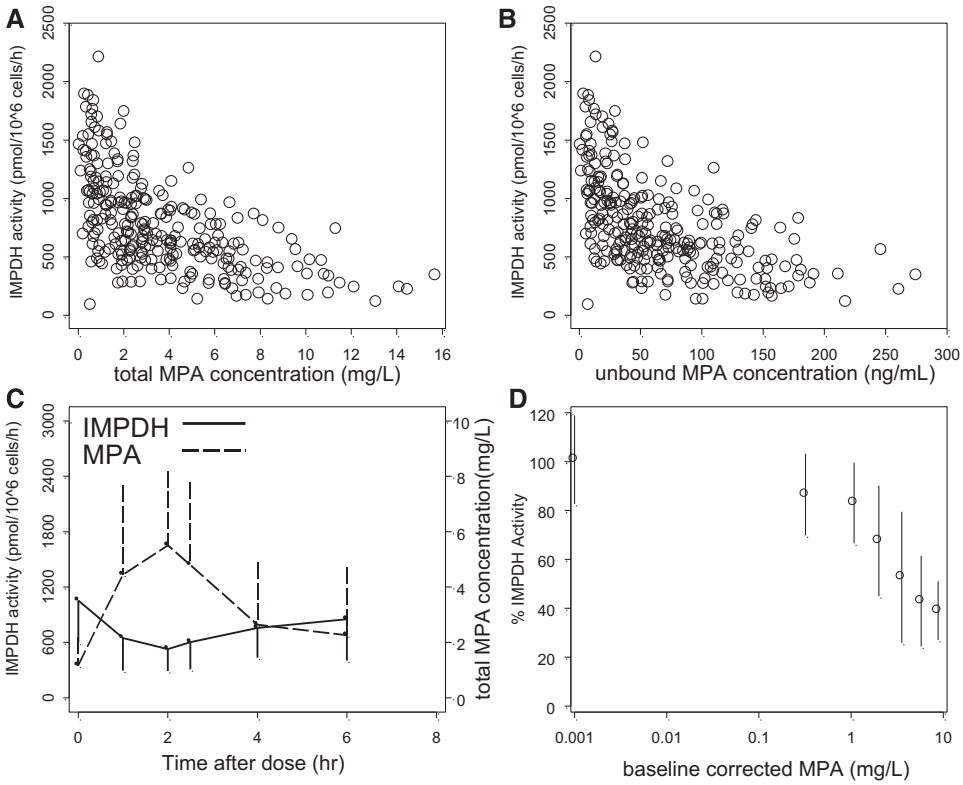

Figure 2. Interpatient variability in IMPDH activity in PMNCs on day +21. Concentration-response of IMPDH activity by total MPA (A) and unbound MPA (B) plasma concentrations. Time course of IMPDH activity and total MPA concentration (mean ± SD) (C). Percentage of IMPDH activity (mean ± SD) vs. total MPA corrected for baseline (ie, predose) values (D).

demonstrated that the population pharmacokinetic-dynamic model accurately predicted the observed MPA pharmacokinetics and IMPDH activity in a separate cohort of HCT participants. For the population prediction, the MPE% for total MPA, unbound MPA, total MPAG, and IMPDH activity were 28.9%, 10.6%, 27.1%, and −1.85%, respectively. For individual Bayesian predictions, MPE% for total MPA, unbound MPA, total MPAG, and IMPDH activity were 4.85%, −2.0%, .4%, and −.97%, respectively. As shown in Supplemental Figure 6, most validation data fall within the 95% confidence interval of the predicted values that were derived from the pharmacokinetic-dynamic parameters estimated from the development dataset.

Pharmacodynamic Relationships

We also sought to evaluate if clinical outcomes could be predicted by the day +21 IMPDH AUEC. The analysis was adjusted for Kahl relapse risk category, female donor to male recipient, and donor type (unrelated versus related). As shown in Table 4, Figure 3, and Supplemental Figure 7, day +21 IMPDH AUEC was associated with CMV reactivation ($P = .003$), nonrelapse mortality ($P = .04$), and overall survival ($P = .03$).

DISCUSSION

The translational relevance of this work is that we created a pharmacokinetic-dynamic model that characterizes the relationship between IMPDH activity with plasma MPA concentrations after oral MMF administration in non-myeloablative HCT patients. Our key results are as follows: (1) weight-based dosing of MMF results in considerable interpatient variability in the inhibition of IMPDH activity, (2) a previous MPA population pharmacokinetic model in HCT recipients has been validated [6], and (3) a population pharmacokinetic-dynamic model of MPA concentrations with IMPDH activity has been developed and validated. No clinical covariates were found for the pharmacodynamic parameters (Supplemental Figure 5), indicating that IMPDH

Table 3
Population Pharmacodynamics Parameters Describing Relationship between Total or Unbound MPA Concentrations and IMPDH Activity on Day +21 in Nonmyeloablative HCT Recipients Taking MMF

Parameter	Explanation	Estimates* (RSE%)† for	
		IMPDH Activity (pmol XMP/10^6 cells/h)	
E_0	Baseline IMPDH activity (immediately before day +21 MMF dose)	1370 (5.6)	
		Total MPA (mg/L)	Unbound MPA (ng/mL)
IC_{50}	MPA concentration causing 50% maximal inhibition	3.23 (10.7)	57.3 (11.2)
IIV_E_0 (CV%)	Interindividual variability of E_0	27.6 (30.8)	27.3 (31.4)
IIV_IC_{50} (CV%)	Interindividual variability of IC_{50}	53.1 (34.2)	56.3 (33.4)
Proportional residual error (%)		.20 (19.3)	.20 (19.3)

CV indicates coefficient of variation; RSE, relative standard error.

* Maximum inhibition could not be estimated based on observed data and therefore was fixed to 1. Hill coefficient was estimated close to 1 and was fixed to 1 in the final parameter estimation.

† The base model is the final model, because none of the evaluated covariates met the criteria for inclusion in the pharmacodynamic model.

Table 4
Association of Day +21 IMPDH AUEC with HCT Outcomes

	Events*	Odds Ratio/ Hazard Ratio† (95% Confidence Interval)	*P*
Day +28 T cell chimerism ≥ 95%	23	.96 (.4-2.6)	.96
Grades II-IV acute GVHD	33	.72 (.4-1.3)	.26
Grades III-IV acute GVHD	4	.13 (.0-1.0)	.05
Extensive chronic GVHD	30	1.38 (.7-2.9)	.38
Relapse	10	.95 (.3-3.2)	.93
CMV reactivation	20	.29 (.1-.7)	.003
Nonrelapse mortality	9	.23 (.1-1.0)	.04
Overall mortality	17	.40 (.2-.9)	.03

* Events on or after day +26.
† Day +28 T cell chimerism analyzed as binary endpoint (odds ratio), and all others as time-to-event endpoint (hazard ratio). Odds ratio and hazard ratio are effects per doubling of IMPDH AUEC. All analyses adjusted for Kahl relapse risk category (low, standard, high), donor–recipient gender (female to male, other), and donor (related, unrelated).

activity should be directly measured and that further research is needed to explain pharmacodynamic variability. IMPDH AUEC on day +21 was associated with CMV reactivation, nonrelapse mortality, and overall mortality (Table 4). These findings should be confirmed in a larger patient population, with the long-term goal of using IMPDH activity in PMNC as a predictive biomarker to improve survival.

The immunosuppressant MMF is an integral component of postgrafting immunosuppression after HCT. HCT recipients receiving MMF dosed by body weight have varying clinical outcomes [21]. We recently constructed MPA population pharmacokinetic models after intravenous MMF [5] or oral MMF [6] administration that revealed considerable IIV in MPA pharmacokinetics. We validated this pharmacokinetic model and refined it by adding concentration-time data of unbound MPA and total MPAG. Oral MMF dosed based on body weight still results in considerable interpatient variability in ex vivo IMPDH activity in PMNCs isolated from participants receiving the same 15-mg/kg dose of oral MMF (Figures 2 and 4). An inhibitory E_{max} model adequately described the inhibition of IMPDH activity in PMNCs by MPA. The IIV of the pharmacodynamic parameters varied from 27.3% to 56.3% (Table 3). This IIV is greater than the IIV of many pharmacokinetic parameters with the notable exception of the IIV of the volume estimates, which range from 47% to 86.4% (Table 2). The large IIV in the volume estimates could be attributed to the inability to accurately characterize the maximum MPA concentration due to the use of a limited sampling schedule, which is a necessity in this patient population treated in the ambulatory clinic.

We hypothesized that estimating its drug-specific pharmacodynamics (IMPDH activity in PMNCs) could be a predictive measure of an individual's response to MMF. Determining IMPDH activity may provide a direct

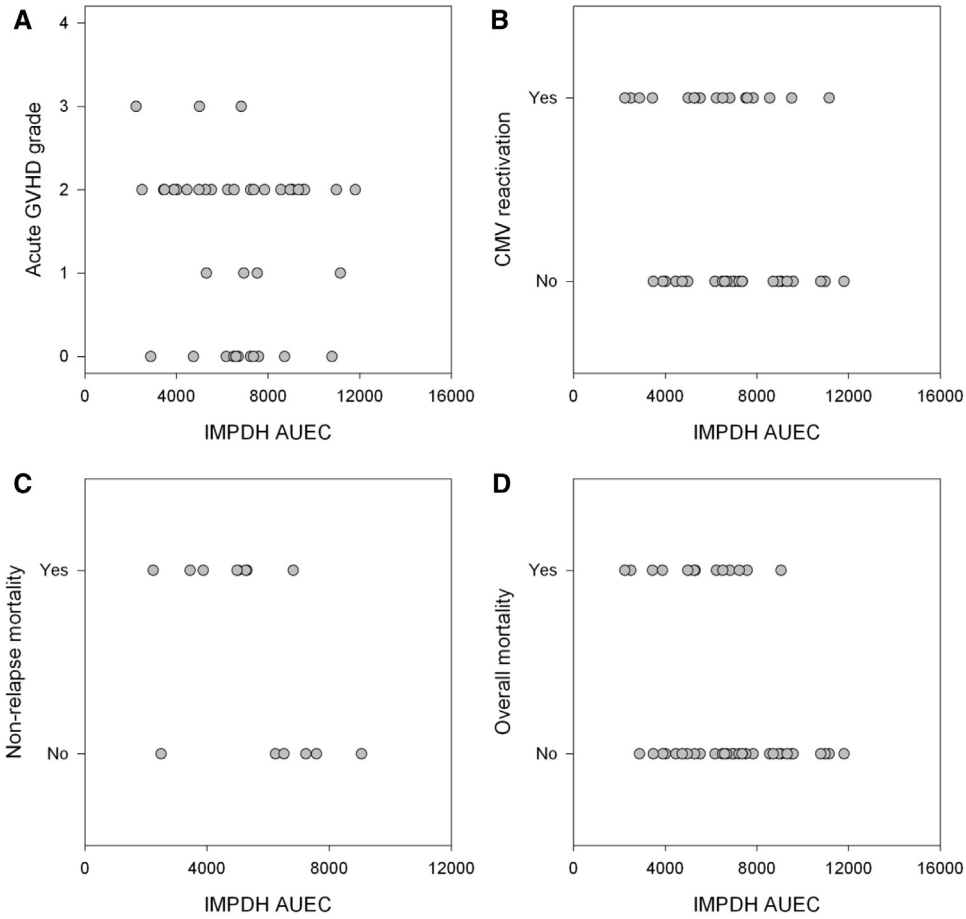

Figure 3. Association of IMPDH AUEC (pmol × 10^6 cells) with acute GVHD (A), CMV reactivation (B), nonrelapse mortality (C), and overall mortality (D) in 45 patients receiving an unrelated donor graft. Only events on or after day +26 are included.

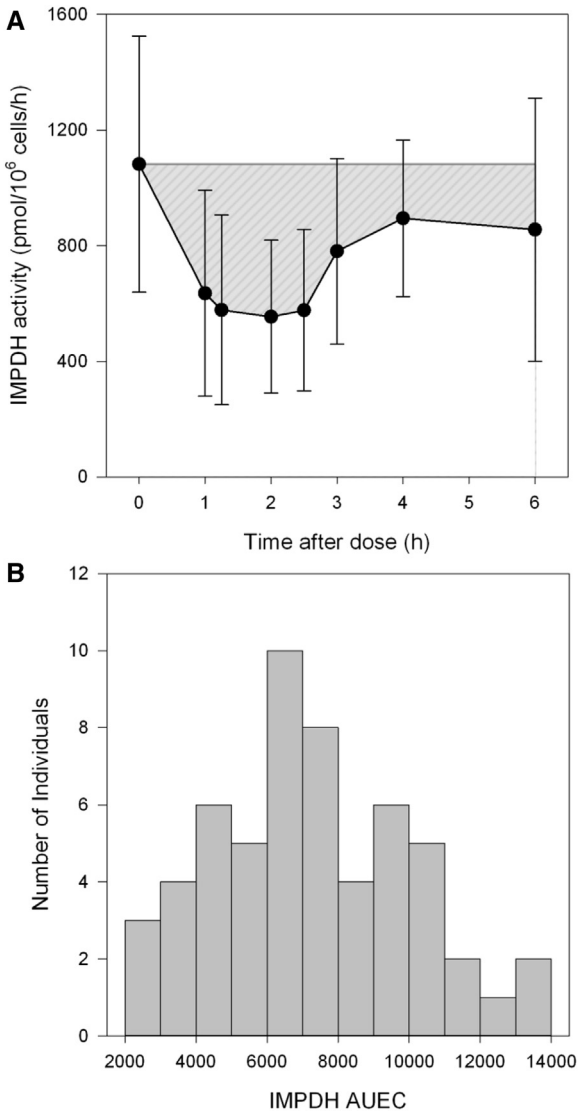

Figure 4. Visual representation of IMPDH AUEC (gray area, in units of pmol × 10^6 cells) after a single dose of MMF at steady state (A) and distribution of IMPDH AUEC in all patients (B).

quantitative method to evaluate the degree of MMF-induced immunosuppression and subsequent clinical efficacy and toxicity. Notably, on day +21, the PMNCs can be derived from the recipient, a mixture of donor and recipient cells, or solely donor cells. The day +28 donor T cell chimerism is presented in Table 1; most patients had >95% T cell chimerism. Variability in the cellular uptake and activation of MPA in PMNCs may account for this differential cellular sensitivity. Notably, concomitant calcineurin inhibitor and graft source were not associated with the IC_{50} and E_{max} of IMPDH inhibition, suggesting these factors do not influence sensitivity to MMF (Supplemental Figure 5).

To our knowledge, this publication is the first to evaluate the association of IMPDH activity after MMF administration in nonmyeloablative HCT recipients. Within HCT recipients, Laverdière et al. [11] characterized IMPDH activity in 19 HCT recipients whose conditioning regimen, graft source, and MMF regimen were not detailed. These investigators reported a 5.3-fold variability in IMPDH activity; our results show a 10-fold variability in IMPDH activity (Figure 2A and B) and 6-fold variability in IMPDH AUEC (Figure 4B). Although we developed a validated LC/MS method to quantitate IMPDH activity, we could not quantitate IMPDH activity on day +2 because of extremely low white blood cell counts, predominantly due to fludarabine/total body irradiation conditioning.

In conclusion, we have shown that adequate number of PMNC can be isolated from HCT recipients on day +21 to quantitate XMP, and thus IMPDH activity, using our highly sensitive assay. We presented an integrated population-based model of total MPA, unbound MPA, and total MPAG plasma concentrations and the associated degree of immunosuppression, as quantified by IMPDH activity in PMNCs. The final model captured the central tendencies and IIV well; there were, however, no clinical covariates associated with the pharmacodynamic parameters. Such a model provides an approach toward individualized oral MMF dosing and a firm rationale for further studies investigating whether dosing MMF on the basis of IMPDH activity can improve clinical outcomes. Subsequent translational studies will be necessary to evaluate whether IMPDH activity after MPA provides a novel biomarker to predict an individual's sensitivity and response to MMF, with the long-range goal of individualizing postgrafting immunosuppression and/or MMF doses to improve the efficacy and/or decrease the toxicity of nonmyeloablative HCT.

ACKNOWLEDGMENTS

The authors are very grateful to the patients who participated in this study. The authors also wish to thank all physicians, nurses, and support personnel for their care of patients on this study.

Financial disclosure: Supported in part by grants HL91744, CA18029, CA78902, HL36444, and HL093294 from the National Heart Lung and Blood Institute and the National Cancer Institute.

Conflict of interest statement: There are no conflicts of interest to report.

SUPPLEMENTARY DATA

Supplementary data related to this article can be found online at http://dx.doi.org/10.1016/j.bbmt.2014.03.032.

REFERENCES

1. Deeg HJ, Maris MB, Scott BL, Warren EH. Optimization of allogeneic transplant conditioning: not the time for dogma. *Leukemia*. 2006;20:1701-1705.
2. Maris MB, Niederwieser D, Sandmaier BM, et al. HLA-matched unrelated donor hematopoietic cell transplantation after nonmyeloablative conditioning for patients with hematologic malignancies. *Blood*. 2003;102:2021-2030.
3. Nash RA, Johnston L, Parker P, et al. A phase I/II study of mycophenolate mofetil in combination with cyclosporine for prophylaxis of acute graft-versus-host disease after myeloablative conditioning and allogeneic hematopoietic cell transplantation. *Biol Blood Marrow Transplant*. 2005;11:495-505.
4. Staatz CE, Tett SE. Clinical pharmacokinetics and pharmacodynamics of mycophenolate in solid organ transplant recipients. *Clin Pharmacokinet*. 2007;46:13-58.
5. Li H, Mager DE, Bemer MJ, et al. A limited sampling schedule to estimate mycophenolic acid area under the concentration-time curve in hematopoietic cell transplantation recipients. *J Clin Pharmacol*. 2011;52:1654-1664.
6. Li H, Mager DE, Sandmaier BM, et al. Population pharmacokinetics and dose optimization of mycophenolic acid in HCT recipients receiving oral mycophenolate mofetil. *J Clin Pharmacol*. 2013;53:393-402.
7. McDermott CL, Sandmaier BM, Storer B, et al. Nonrelapse mortality and mycophenolic acid exposure in nonmyeloablative hematopoietic cell transplantation. *Biol Blood Marrow Transplant*. 2013;19:1159-1166.
8. Haentzschel I, Freiberg-Richter J, Platzbecker U, et al. Targeting mycophenolate mofetil for graft-versus-host disease prophylaxis after

allogeneic blood stem cell transplantation. *Bone Marrow Transplant*. 2008;42:113-120.
9. Kuypers DR, Le Meur Y, Cantarovich M, et al. Consensus report on therapeutic drug monitoring of mycophenolic acid in solid organ transplantation. *Clin J Am Soc Nephrol*. 2010;5:341-358.
10. Allison AC, Eugui EM. Mycophenolate mofetil and its mechanisms of action. *Immunopharmacology*. 2000;47:85-118.
11. Laverdière I, Caron P, Couture F, et al. Liquid chromatography-coupled tandem mass spectrometry based assay to evaluate inosine-5'-monophosphate dehydrogenase activity in peripheral blood mononuclear cells from stem cell transplant recipients. *Anal Chem*. 2012;84:216-223.
12. Bemer MJ, Sorror M, Sandmaier BM, et al. A pilot pharmacologic biomarker study in HLA-haploidentical hematopoietic cell transplant recipients. *Cancer Chemother Pharmacol*. 2013;72:607-618.
13. Glander P, Sombogaard F, Budde K, et al. Improved assay for the nonradioactive determination of inosine 5'-monophosphate dehydrogenase activity in peripheral blood mononuclear cells. *Ther Drug Monit*. 2009;31:351-359.
14. Daxecker H, Raab M, Muller MM. Influence of mycophenolic acid on inosine 5'-monophosphate dehydrogenase activity in human peripheral blood mononuclear cells. *Clin Chim Acta*. 2002;318:71-77.
15. Musuamba FT, Rousseau A, Bosmans JL, et al. Limited sampling models and Bayesian estimation for mycophenolic acid area under the curve prediction in stable renal transplant patients co-medicated with ciclosporin or sirolimus. *Clin Pharmacokinet*. 2009;48:745-758.
16. Bullingham RE, Nicholls AJ, Kamm BR. Clinical pharmacokinetics of mycophenolate mofetil. *Clin Pharmacokinet*. 1998;34:429-455.
17. Przepiorka D, Weisdorf D, Martin P, et al. 1994 Consensus Conference on Acute GVHD Grading. *Bone Marrow Transplant*. 1995;15:825-828.
18. Kahl C, Storer BE, Sandmaier BM, et al. Relapse risk in patients with malignant diseases given allogeneic hematopoietic cell transplantation after nonmyeloablative conditioning. *Blood*. 2007;110:2744-2748.
19. Feng HY, Liu WB, Huang X, et al. [Efficacy and safety of low-dose cyclophosphamide plus corticosteroids for type I/II myasthenia gravis]. *Zhonghua Yi Xue Za Zhi*. 2012;92:2323-2326.
20. Gabrielsson J, Weiner D. *Pharmacokinetic and pharmacodynamic data analysis: concepts and applications*. Stockholm Sweden: Swedish Pharmaceutical Press; 2007.
21. McDermott CL, Sandmaier BM, Storer B, et al. Non-relapse mortality and mycophenolic acid exposure in nonmyeloablative hematopoietic cell transplantation. *Biol Blood Marrow Transplant*. 2013 Aug;19(8):1159-1166.